Effect of Local Coordination on the Photoluminescence Properties of Er-doped Y_2O_3 Thin Films

Miniaturizing the erbium-doped optical fiber amplifier (~20 m in length) into a small, compact amplifier that can be integrated with other optical and electronic devices on a single chip (optoelectronics) offers great promise in optical communication as an alternative to the electronic technology.[i,ii] The gain of these miniaturized devices is limited by the solubility, concentration, and distribution of optically-active Er^{3+} in a host material.[iii] While incorporation of a high concentration of erbium is possible by ion implantation, the method does not allow for the control of spatial distribution or the activation of the ions in the host. This is critical at high Er concentrations, since non-radiative processes resulting from ion-ion interactions become dominant and significantly reduce the photoluminescence (PL) yield.

In this work, we demonstrated radical-enhanced atomic layer deposition (RE-ALD) as a viable technique to synthesize Er^{3+}-doped dielectric thin films with a precise control of its concentration and spatial distribution, thus tailoring the PL property of Er^{3+} doped waveguides. Since the optically-active Er needs to be in the trivalent state, showing highest photoluminescence efficiency when coordinating with approximately six O atoms as in crystalline Er_2O_3, Y_2O_3 was chosen as the host material due to its identical crystal structure and very similar lattice constant to Er_2O_3.[IV-V] In this case, typical problems such as lattice distortion and vacancy formation which are detrimental to the PL yield can essentially be eliminated. The thin film deposition was carried out in an ultra-high vacuum multi-beam reactor in which metal β-diketonate complexes and oxygen radicals were introduced independently and sequentially. Incorporation of Er in Y_2O_3 thin films at 350°C was accomplished by combining the self-limiting RE-ALD of Y_2O_3 and Er_2O_3 in an alternating fashion, with the Er doping level at a specific depth location controlled by varying the ratio of Y_2O_3:Er_2O_3 cycles during deposition.
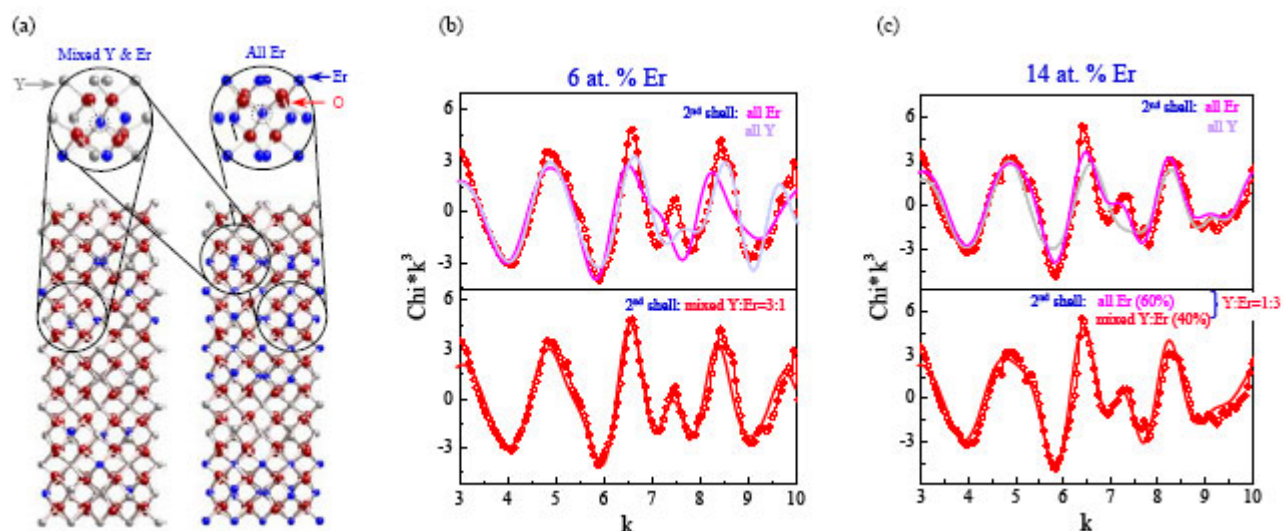

Figure 1: (a) Proposed structures of Y_2O_3 films doped with low and high concentrations of Er^{3+}, (b) EXAFS analysis of a 6 at.% Er^{3+} doped Y_2O_3 thin film, and (c) EXAFS analysis of a 14 at.% Er^{3+} doped Y_2O_3 thin film.

The nanostructure of Er-doped Y_2O_3 thin films was investigated by using a high-resolution transmission electron microscopy (HRTEM) and electron energy loss spectrometry (EELS). Specifically, the distribution of Er separated by layers of Y_2O_3 was confirmed by elemental EELS

mapping of Er M_4 and M_5, with the Er concentration controlled from 6 to 14 at.%, determined by X-ray photoelectron spectroscopy (XPS). This unique feature is characteristic of the alternating RE-ALD of Y_2O_3 and Er_2O_3. The photoluminescence yield was found to reduce by at least one order of magnitude when the Er doping level exceeded 8 at.%. This photoluminescence quenching, also commonly known as *concentration quenching*, is attributed to two main processes: Er immiscibility in the host matrix and/or Er ion-ion interaction. To delineate the origin of this photoluminescence reduction, we applied X-ray absorption near-edge spectroscopy (XANES) and extended X-ray absorption fine structure (EXAFS) analyses.

X-ray absorption near edge spectroscopy (XANES) study using the Er L_{III} edge at 8358 eV confirmed that Er was in the optically active trivalent state (Er^{3+}), having an octahedral symmetry similar to Er in Er_2O_3. No other chemical state was found up to at least 14 at.%, indicating no formation of Er precipitate which is optically inactive. To obtain further insight into the Er local coordination, three different 4-Å local cluster models were constructed, corresponding to three different possible Er configurations in the Y_2O_3 thin film. In all three models, the first shell is O while the second shell can be all Er^{3+} (first model), all Y^{3+} (second model), or a mixture of Y^{3+} and Er^{3+} (third model). Because of the almost perfect crystal structure match between Y_2O_3 and Er_2O_3, the simulation of the Er-doped Y_2O_3 local structure was simply accomplished by replacing Y^{3+} with Er^{3+} in the Y_2O_3 lattice. Shown in Figure 1a (left) is a pictorial view of the Er-doped Y_2O_3 structure at low Er concentration. In this case, the center absorbing Er has a second coordination shell with a mixture of both Er and Y. At high Er concentration where the alternating growth of Y_2O_3 and Er_2O_3 resulting in an exsolution with Er_2O_3-rich domains (Figure 1a, right), the Er local environment is described by combining the first and third model.

Shown in Figure 1b are the k^3-weighted EXAFS of the Y_2O_3 thin films doped with 6 at.% Er, representing samples with high photoluminescence yield. The best fit to the EXAFS using the 1st and 2nd model agreed fairly well with the EXAFS up to $k \sim 6$ Å^{-1}, mainly from the first O shell, but failed to describe the oscillations at higher k (Figure 1b top). This indicates that the second nearest neighbors are neither all Er^{3+} in which case the local environment of Er^{3+} would be similar to that of Er^{3+} in Er_2O_3, nor all Y^{3+} which would otherwise indicate an infinite dilution of Er^{3+} in Y_2O_3. A best fit to the EXAFS was achieved with the third model (Figure 1b bottom) when the Y:Er cation ratio is specified to be 3:1, as determined by XPS compositional analysis In this case, a coordination number of 6 for the first O shell and 8-9 for the second shell were obtained. Furthermore, Er^{3+} was found to be completely miscible in the Y_2O_3 matrix up to at least 8 at.%, showing no evidence of Y_2O_3 and Er_2O_3 phase segregation. There is also no indication of Er−Er coordination within 4-Å proximity.

For the 14 at.% Er-doped Y_2O_3 thin film, representing samples with low photoluminescence yield, a combination of the first (~60%) and third model (~40%) best fitted the EXAFS spectrum (Figure 1c), with the Y:Er cation ratio specified at 1:3, as determined by XPS. This is consistent with the alternating RE-ALD process, resulting in a layer-like structure under these deposition conditions. Since there is no indication of Er-Er coordination in all samples doped with 6 to 14 at.% Er^{3+}, it is concluded that the photoluminescence quenching observed in samples with Er concentration exceeding 8 at.% is not due to Er immiscibility in Y_2O_3 but likely due to Er ion-ion interaction. When the Er^{3+} concentration is sufficiently small, the ions are evenly distributed in the Y_2O_3 matrix with relatively large inter-ionic distances, impeding ion-ion interaction. Consequently, the photoluminescence yield is relatively high in the absence of these competing processes. As the Er^{3+} concentration increases, there is more Er^{3+} within a 4-Å proximity of each other that they can interact, resulting in cooperative energy upconversion or energy migration, leading to reduced photoluminescence yield.

Using EXAFS, the origin of the observed concentration quenching of photoluminescence for the Er^{3+}:Y_2O_3 system was delineated. The study also suggests that, in order to prevent ion-ion

interaction, no Er^{3+} should have another Er^{3+} as a second nearest neighbor. This criteria sets an upper limit on the Er^{3+} concentration in the Y_2O_3 host at $\sim 6\times10^{21}/cm^3$, or ~10 at.%, estimated by systematically replacing Y^{3+} in the Y_2O_3 unit cell by Er^{3+} while ensuring there is no direct $Er-O-Er$ bonding.   These results are essential to the understanding of the Er^{3+} optical properties in correlation to its local structure, allowing for the optimization of the photoluminescence yield by controlling its distribution in the host lattice.

Primary Citation

T.T. Van, Bargar, J.R., and Chang, J.P. (2006) Structural investigation of Er coordination in Y_2O_3. J. Applied Physics 100, 023115

References

[i] E. Desurvire, *Erbium-doped Fiber Amplifiers: Principles and Applications* (John Wiley & Sons, Inc., New York, 1994).

[ii] A. Polman and F. C. J. M van Veggel, J. Opt. Soc. Am. B 21, 871 (2004).

[iii] F. Auzel, in *Spectroscopic Properties of Rare Earths in Optical Materials*, 1st edition, edited by G. Liu & B. Jacquier (Springer, New York, 2005), Vol. 83, Chap. 5, p.266.

[IV] D. J. Eaglesham, J. Michel, E. A. Fitzgerald, D. C. Jacobson, and J. M. Poate, Appl. Phys. Lett. 58, 2797 (1991).

[V] E. C. M. Pennings, G. H. Manhoudt, and M. K. Smit, Electron. Lett. 24, 998 (1988).